

# Purcell effect in sub-wavelength semiconductor lasers

Qing Gu,<sup>1,\*</sup> Boris Slutsky,<sup>1</sup> Felipe Vallini,<sup>2</sup> Joseph S. T. Smalley,<sup>1</sup> Maziar P. Nezhad,<sup>1,3</sup> Newton C. Frateschi,<sup>2</sup> and Yeshaiah Fainman<sup>1</sup>

<sup>1</sup>Department of Electrical and Computer Engineering, University of California at San Diego, La Jolla, CA, 92093-0407, USA

<sup>2</sup>Department of Applied Physics, "Gleb Wataghin" Physics Institute, University of Campinas - UNICAMP, 13083-859 Campinas, SP, Brazil

<sup>3</sup>Currently with Integrated Photonics Group, RWTH Aachen University, Sommerfeldstr. 24, 52074 Aachen, Germany  
[\\*qigu@ucsd.edu](mailto:qigu@ucsd.edu)

**Abstract:** We present a formal treatment of the modification of spontaneous emission rate by a cavity (Purcell effect) in sub-wavelength semiconductor lasers. To explicitly express the assumptions upon which our formalism builds, we summarize the results of non-relativistic quantum electrodynamics (QED) and the emitter-field-reservoir model in the quantum theory of damping. Within this model, the emitter-field interaction is modified to the extent that the field mode is modified by its environment. We show that the Purcell factor expressions frequently encountered in the literature are recovered only in the hypothetical condition when the gain medium is replaced by a transparent medium. Further, we argue that to accurately evaluate the Purcell effect, both the passive cavity boundary and the collective effect of all emitters must be included as part of the mode environment.

©2013 Optical Society of America

**OCIS codes:** (140.5960) Semiconductor lasers; (270.5580) Quantum electrodynamics; (140.3948) Microcavity devices.

---

## References and links

1. S. Haroche, "New trends in atomic physics," in *Proceedings of the Les Houches Summer School of Theoretical Physics, Session XXXVIII, 1982*, G. Grynberg and R. Stora, ed. (Elsevier Science, 1984), pp. 195–309.
2. H. Walther, "Experiments on cavity quantum electrodynamics," *Phys. Rep.* **219**(3-6), 263–281 (1992).
3. E. M. Purcell, "Spontaneous emission probabilities at radio frequencies," *Phys. Rev.* **69**, 681 (1946).
4. J. M. Gérard and B. Gayral, "Strong Purcell effect for InAs quantum boxes in three-dimensional solid-state microcavities," *J. Lightwave Technol.* **17**(11), 2089–2095 (1999).
5. P. Yu, P. Bhattacharya, and J. Cheng, "Enhanced spontaneous emission from InAs/GaAs self-organized quantum dots in a GaAs photonic-crystal-based microcavity," *J. Appl. Phys.* **93**(10), 6173–6176 (2003).
6. T. Baba and D. Sano, "Low-threshold lasing and Purcell effect in microdisk lasers at room temperature," *IEEE J. Sel. Top. Quantum Electron.* **9**(5), 1340–1346 (2003).
7. M. T. Hill, Y. S. Oei, B. Smalbrugge, Y. Zhu, T. De Vries, P. J. van Veldhoven, F. W. M. van Otten, T. J. Eijkemans, J. P. Turkiewicz, H. de Waardt, E. J. Geluk, S.-H. Kwon, Y.-H. Lee, R. Nötzel, and M. K. Smit, "Lasing in metallic-coated nanocavities," *Nat. Photonics* **1**(10), 589–594 (2007).
8. M. P. Nezhad, A. Simic, O. Bondarenko, B. Slutsky, A. Mizrahi, L. Feng, V. Lomakin, and Y. Fainman, "Room-temperature subwavelength metallo-dielectric lasers," *Nat. Photonics* **4**(6), 395–399 (2010).
9. K. Ding and C. Ning, "Metallic subwavelength-cavity semiconductor nanolasers," *Light: Sci. Appl.* **1**(7), e20 (2012).
10. Y. Xu, J. Vučković, R. Lee, O. Painter, A. Scherer, and A. Yariv, "Finite-difference time-domain calculation of spontaneous emission lifetime in a microcavity," *J. Opt. Soc. Am. B* **16**(3), 465–474 (1999).
11. H. Y. Ryu and M. Notomi, "Enhancement of spontaneous emission from the resonant modes of a photonic crystal slab single-defect cavity," *Opt. Lett.* **28**(23), 2390–2392 (2003).
12. T. Suhr, N. Gregersen, K. Yvind, and J. Mørk, "Modulation response of nanoLEDs and nanolasers exploiting Purcell enhanced spontaneous emission," *Opt. Express* **18**(11), 11230–11241 (2010).
13. C. A. Ni and S. L. Chuang, "Theory of high-speed nanolasers and nanoLEDs," *Opt. Express* **20**(15), 16450–16470 (2012).

14. A. Meldrum, P. Bianucci, and F. Marsiglio, "Modification of ensemble emission rates and luminescence spectra for inhomogeneously broadened distributions of quantum dots coupled to optical microcavities," *Opt. Express* **18**(10), 10230–10246 (2010).
15. C. Cohen-Tannoudji, J. Dupont-Roc, and G. Grynberg, *Photons and Atoms: Introduction to Quantum Electrodynamics* (Wiley, 1989).
16. J. J. Sakurai, *Modern quantum mechanics* (Addison-Wesley, 1994).
17. R. J. Glauber and M. Lewenstein, "Quantum optics of dielectric media," *Phys. Rev. A* **43**(1), 467–491 (1991).
18. S. W. Chang and S. L. Chuang, "Normal modes for plasmonic nanolasers with dispersive and inhomogeneous media," *Opt. Lett.* **34**(1), 91–93 (2009).
19. S. W. Chang and S. L. Chuang, "Fundamental formulation for plasmonic nanolasers," *IEEE J. Quantum Electron.* **45**(8), 1014–1023 (2009).
20. M. O. Scully and M. S. Zubairy, *Quantum optics* (Cambridge University, 1997).
21. M. Asada, "Intraband relaxation time in quantum-well lasers," *IEEE J. Quantum Electron.* **25**(9), 2019–2026 (1989).
22. R. J. Glauber, "Optical Coherence and Photon Statistics" in *Quantum Optics and Electronics* (Les Houches, 1965).
23. L. A. Coldren and S. W. Corzine, *Diode lasers and photonic integrated circuits* (John Wiley & Sons, inc., 1995).
24. G. Björk, S. Machida, Y. Yamamoto, and K. Igeta, "Modification of spontaneous emission rate in planar dielectric microcavity structures," *Phys. Rev. A* **44**(1), 669–681 (1991).
25. K. Srinivasan and O. Painter, "Linear and nonlinear optical spectroscopy of a strongly coupled microdisk-quantum dot system," *Nature* **450**(7171), 862–865 (2007).
26. G. Khitrova, H. Gibbs, M. Kira, S. Koch, and A. Scherer, "Vacuum Rabi splitting in semiconductors," *Nat. Phys.* **2**(2), 81–90 (2006).
27. V. Weisskopf and E. Wigner, "Calculation of the natural brightness of spectral lines on the basis of Dirac's theory," *Z. Phys.* **63**, 54–73 (1930).
28. A. Yariv and P. Yeh, *Photonics: Optical Electronics in Modern Communications* (Oxford University, 2007).
29. A. E. Siegman, *An introduction to lasers and masers* (McGraw Hill, 1971).
30. G. P. Agrawal and N. A. Olsson, "Self-phase modulation and spectral broadening of optical pulses in semiconductor laser amplifiers," *IEEE J. Quantum Electron.* **25**(11), 2297–2306 (1989).
31. H. J. Carmichael, *Statistical Methods in Quantum Optics 1: Master Equations and Fokker-Planck Equations* (Springer-Verlag, 1999).
32. T. Baba, D. Sano, K. Nozaki, K. Inoshita, Y. Kuroki, and F. Koyama, "Observation of fast spontaneous emission decay in GaInAsP photonic crystal point defect nanocavity at room temperature," *Appl. Phys. Lett.* **85**(18), 3989–3991 (2004).
33. H. Iwase, D. Englund, and J. Vucković, "Analysis of the Purcell effect in photonic and plasmonic crystals with losses," *Opt. Express* **18**(16), 16546–16560 (2010).
34. M. Fujita, A. Sakai, and T. Baba, "Ultrasmall and ultralow threshold GaInAsP-InP microdisk injection lasers: design, fabrication, lasing characteristics, and spontaneous emission factor," *IEEE J. Sel. Top. Quantum Electron.* **5**(3), 673–681 (1999).
35. H. Altug, D. Englund, and J. Vučković, "Ultrafast photonic crystal nanocavity laser," *Nat. Phys.* **2**(7), 484–488 (2006).
36. M. Glauser, G. Rossbach, G. Cosendey, J. Levrat, M. Cobet, J. Carlin, J. Besbas, M. Gallart, P. Gilliot, R. Butté, and N. Grandjean, "Investigation of InGaN/GaN quantum wells for polariton laser diodes," *Phys. Status Solidi C* **9**(5), 1325–1329 (2012).
37. M. Yamada and Y. Suematsu, "Analysis of gain suppression in undoped injection lasers," *J. Appl. Phys.* **52**(4), 2653–2664 (1981).
38. M. Khajavikhan, A. Simic, M. Katz, J. H. Lee, B. Slutsky, A. Mizrahi, V. Lomakin, and Y. Fainman, "Thresholdless nanoscale coaxial lasers," *Nature* **482**(7384), 204–207 (2012).
39. M. Yamanishi and Y. Lee, "Phase dampings of optical dipole moments and gain spectra in semiconductor lasers," *IEEE J. Quantum Electron.* **23**(4), 367–370 (1987).
40. S. R. Chinn, P. Zory, Jr., and A. R. Reisinger, "A model for GRIN-SCH-SQW diode lasers," *IEEE J. Quantum Electron.* **24**(11), 2191–2214 (1988).
41. B. Deveaud, F. Clérot, N. Roy, K. Satzke, B. Sermage, and D. S. Katzer, "Enhanced radiative recombination of free excitons in GaAs quantum wells," *Phys. Rev. Lett.* **67**(17), 2355–2358 (1991).
42. W. W. Chow and S. W. Koch, *Semiconductor-laser fundamentals* (Springer, 1999).
43. D. Martín-Cano, A. González-Tudela, L. Martín-Moreno, F. J. García-Vidal, C. Tejedor, and E. Moreno, "Dissipation-driven generation of two-qubit entanglement mediated by plasmonic waveguides," *Phys. Rev. B* **84**(23), 235306 (2011).
44. W. Kowalsky, A. Schlachetzki, and F. Fiedler, "Near-band-gap absorption of InGaAsP at 1.3  $\mu\text{m}$  wavelength," *Phys. Status Solidi A* **68**(1), 153–158 (1981).
45. R. H. Groeneveld, R. Sprik, and A. Lagendijk, "Effect of a nonthermal electron distribution on the electron-phonon energy relaxation process in noble metals," *Phys. Rev. B Condens. Matter* **45**(9), 5079–5082 (1992).
46. W. S. Fann, R. Storz, H. W. Tom, and J. Bokor, "Electron thermalization in gold," *Phys. Rev. B Condens. Matter* **46**(20), 13592–13595 (1992).

## 1. Introduction

The fundamental system in cavity quantum electrodynamics (cavity-QED) is a two-level emitter interacting with the electromagnetic field in a cavity [1,2]. Characteristics of this system, such as the spontaneous decay rate, are not inherent to the emitter, but depend on the interaction between the emitter and cavity modes. Further, the emitter-mode interactions undergo modifications as the cavity modes are modified by their environment, for example the lossy boundaries of a non-ideal cavity.

The spontaneous emission rate of an emitter in a cavity may be enhanced or inhibited compared to emission in free space, a phenomenon known as the Purcell effect [3]. The spontaneous emission modification factor, also known as the Purcell factor, scales inversely with the cavity mode volume. In nano-scale lasers, enhanced emission together with a reduced number of cavity modes relative to large lasers can have significant effects, especially on sub-threshold behavior. These effects are generally desirable, as they tend to increase the utilization of spontaneous emission into the lasing mode and lower the lasing threshold. Rate equation models of micro- and nano-scale lasers often incorporate the Purcell factor into the spontaneous emission term [4–9].

Since its original description by Purcell, the modification of spontaneous emission has been studied in a number of general physical contexts, such as when the emitter and cavity mode are not on resonance [4,10], when the spectral broadening of the emitter and cavity mode are comparable [11–13], and when the emitters are a collection of non-identical quantum dots (QDs) [14]. In this work, we apply the theory specifically to semiconductor nanolasers such as those reported in Refs [7–9], and include both inhomogeneous broadening (due to the distribution of carrier energies within the conduction and valence bands) and homogeneous broadening (due to intraband scattering). Although part of our formalism is similar to that used in Ref [14] for quantum dots, the underlying physics differ. We summarize the relevant results from cavity-QED and the quantum theory of damping to explicitly express the assumptions upon which our argument rests. We discuss how the assumptions apply or fail to apply in semiconductor nanolasers. In particular, we argue that the spontaneous emission probability of an electron-hole pair in a cavity is modified not only by the cavity itself, but also, though indirectly, by the aggregate of other electron-hole pairs present. This latter effect can be significant, yet is not readily included into existing models.

This paper is organized as follows: In the first section, we summarize the non-relativistic QED theory that forms the basis of our formulation. We then give the general expressions for the spontaneous emission probabilities in free space and in a cavity, assuming the emitters are two-level-systems. In the subsequent sections, we apply the results to semiconductor nanolasers. We obtain the expression of the Purcell factor for semiconductor lasers, accounting for the loss at the cavity boundary, but not for the indirect effect of the aggregate of emitters. In a numerical example, we illustrate our result by evaluating the Purcell effect of a sub-wavelength semiconductor laser reported by Nezhad et al. [8]. For this example, we use an absorptive reservoir because only the cavity boundary is included in the environment. Finally, we discuss the importance of the aggregate emitter effect, and the difficulties it presents within the framework of the current model.

## 2. Non-relativistic QED in free space and in a cavity

Following the formalism of ([15]. §III.A.1), we begin the non-relativistic QED description of the electric field in free space and in a cavity by separating the longitudinal and transverse components of the electric field operator,  $\hat{E} = \hat{E}_{\parallel} + \hat{E}_{\perp}$ . The longitudinal field operator  $\hat{E}_{\parallel}$  is fully determined by the charge distribution and describes the quasi-static field of charged particles. In what follows, we model electron-hole pairs in the gain material as two-level quantum systems, and cavity materials with their macroscopic permittivities  $\epsilon$ ; the model

includes no charged particles. We therefore focus on the source-free condition and ignore  $\hat{E}_{\parallel}$ . The transverse component of a free field is given by ([15], §III.B.2).

$$\hat{E}_{\perp}(\mathbf{r}, t) = \sum_{\mathbf{k}, \boldsymbol{\varepsilon}} \sqrt{\frac{\hbar \omega_{\mathbf{k}}}{2 \varepsilon_0 L^3}} i (\hat{a}_{\mathbf{k}, \boldsymbol{\varepsilon}}(t) e^{i\mathbf{k} \cdot \mathbf{r}} - \hat{a}_{\mathbf{k}, \boldsymbol{\varepsilon}}^{\dagger}(t) e^{-i\mathbf{k} \cdot \mathbf{r}}) \boldsymbol{\varepsilon} \quad (1)$$

In Eq. (1), the summation is over all free space modes,  $\mathbf{k}$  is the wavevector of the mode, and  $\boldsymbol{\varepsilon}$  is the polarization unit vector of the mode, satisfying  $\boldsymbol{\varepsilon} \perp \mathbf{k}$ .  $\omega_{\mathbf{k}} = |\mathbf{k}|c$  is the mode frequency,  $L^3$  is the quantization volume,  $\hat{a}_{\mathbf{k}, \boldsymbol{\varepsilon}}^{\dagger}(t)$  and  $\hat{a}_{\mathbf{k}, \boldsymbol{\varepsilon}}(t)$  are photon creation and annihilation operators for the mode, respectively, and

$$\hat{a}_{\mathbf{k}, \boldsymbol{\varepsilon}}(t) = \hat{a}_{\mathbf{k}, \boldsymbol{\varepsilon}}(0) \cdot e^{-i\omega_{\mathbf{k}} t}, \quad \hat{a}_{\mathbf{k}, \boldsymbol{\varepsilon}}^{\dagger}(t) = \hat{a}_{\mathbf{k}, \boldsymbol{\varepsilon}}^{\dagger}(0) \cdot e^{i\omega_{\mathbf{k}} t} \quad (2)$$

where  $\hat{a}(0)$  and  $\hat{a}^{\dagger}(0)$  are the operator values at time  $t = 0$ . Equations (1) and (2) are written for a free field in the Heisenberg picture, in which quantum states are constant and operators vary with time. They also apply in the Dirac picture for a field interacting with, for example, a two-level emitter if the interaction is included as correction to the un-perturbed Hamiltonian. In this situation, the quantum states evolve due to the interaction ([16], §5.5). It is often convenient to separate Eq. (1) into annihilation  $\hat{E}_{\perp}^{+}$  and creation  $\hat{E}_{\perp}^{-}$  terms,

$$\begin{aligned} \hat{E}_{\perp}(\mathbf{r}, t) &= \hat{E}_{\perp}^{+}(\mathbf{r}, t) + \hat{E}_{\perp}^{-}(\mathbf{r}, t), \\ \hat{E}_{\perp}^{+}(\mathbf{r}, t) &= \sum_{\mathbf{k}, \boldsymbol{\varepsilon}} \sqrt{\frac{\hbar \omega_{\mathbf{k}}}{2 \varepsilon_0 L^3}} i \hat{a}_{\mathbf{k}, \boldsymbol{\varepsilon}}(t) e^{i\mathbf{k} \cdot \mathbf{r}} \boldsymbol{\varepsilon}, \\ \hat{E}_{\perp}^{-}(\mathbf{r}, t) &= (\hat{E}_{\perp}^{+}(\mathbf{r}, t))^{\dagger} = - \sum_{\mathbf{k}, \boldsymbol{\varepsilon}} \sqrt{\frac{\hbar \omega_{\mathbf{k}}}{2 \varepsilon_0 L^3}} i \hat{a}_{\mathbf{k}, \boldsymbol{\varepsilon}}^{\dagger}(t) e^{-i\mathbf{k} \cdot \mathbf{r}} \boldsymbol{\varepsilon} \end{aligned} \quad (3)$$

An analogous representation exists for the electric field operator in a cavity [17,18]. In a source-free cavity, the electric field operator becomes

$$\hat{E}_u(\mathbf{r}, t) = \hat{E}_u^{+}(\mathbf{r}, t) + \hat{E}_u^{-}(\mathbf{r}, t) = \sum_{\omega_k > 0} i \sqrt{\hbar \omega_k} (\hat{a}_k(t) - \hat{a}_k^{\dagger}(t)) \cdot \mathbf{e}_k(\mathbf{r}) \quad (4)$$

where the summation is over all cavity modes and  $\omega_k$  is the eigenfrequency of the mode  $k$ . In Eq. (4),  $\mathbf{r}$  is the location at which the field is evaluated,  $\mathbf{e}_k(\mathbf{r})$  is the electric field modal profile normalized so that the mode energy evaluates to  $\frac{1}{2} \hbar \omega_k (\hat{a}_k(t) \hat{a}_k^{\dagger}(t) + \hat{a}_k^{\dagger}(t) \hat{a}_k(t))$ , i.e.,  $\hbar \omega_k$  per quantum level of the harmonic oscillator and  $\frac{1}{2} \hbar \omega_k$  in the oscillator ground state. Explicitly, in non-dispersive media,

$$\mathbf{e}_k(\mathbf{r}) = \frac{\mathbf{E}_k(\mathbf{r})}{\sqrt{N_k}}, \quad N_k \triangleq \int_V [\boldsymbol{\varepsilon}(\mathbf{r}) \mathbf{E}_k^2(\mathbf{r}) + \mu(\mathbf{r}) \mathbf{H}_k^2(\mathbf{r})] d^3 \mathbf{r} \quad (5)$$

where  $N_k$  is the normalization factor for mode  $k$  and the integration is over the entire volume in space.  $\mathbf{E}_k(\mathbf{r})$  and  $\mathbf{H}_k(\mathbf{r})$  represent real cavity mode fields (solutions of the classical Maxwell's equations for the cavity geometry), and integration is over all space. In electrically dispersive but magnetically non-dispersive media,  $N_k$  becomes [19]

$$\begin{aligned}
N_k &= \int_V \left[ \left. \frac{\partial(\omega' \epsilon_R(\mathbf{r}, \omega'))}{\partial \omega'} \right|_{\omega'=\omega_k} E_k^2(\mathbf{r}) + \mu(\mathbf{r}) H_k^2(\mathbf{r}) \right] d^3\mathbf{r} \\
&= \int_V \left[ \left( \left. \frac{\partial(\omega' \epsilon_R(\mathbf{r}, \omega'))}{\partial \omega'} \right|_{\omega'=\omega_k} + \epsilon_R(\mathbf{r}, \omega_k) \right) E_k^2(\mathbf{r}) \right] d^3\mathbf{r}
\end{aligned} \tag{6}$$

where  $\epsilon_R$  stands for the real part of permittivity  $\epsilon$ . The assumed, non-dispersive magnetic permeability enables us to express the total magnetic energy in Eq. (6) in terms of the electric field [18]. Although  $\epsilon_R$  may be negative in some metallic materials, the integral in Eq. (6) is always positive. Note that the preceding formalism lacks the imaginary part of the permittivity, and therefore ignores damping in the cavity. Damping may be introduced using Heisenberg-Langevin reservoir theory ([20]. §9). We discuss such an approach to damping in the rest of this section.

When the electromagnetic mode interacts with the environment, the time dependence of  $\hat{a}_k(t)$  and  $\hat{a}_k^\dagger(t)$  can no longer be described by Eq. (2). A damping environment can often be modeled as a thermal reservoir. The reservoir model is applicable when the interaction is weak and the environment is a large stochastic system that satisfies the Markovian approximation, namely, a system that over a short time  $\tau_{\text{reservoir}}$  becomes fully disordered and loses all memory of its earlier state. Intuitively, the interaction must be sufficiently weak and the reservoir characteristic time  $\tau_{\text{reservoir}}$  sufficiently short, so the mode experiences all possible states of the reservoir in equal measure. The reservoir formalism will be employed in Section 4 to describe loss at the boundary of the cavity. Hereafter the terms environment and reservoir are used interchangeably.

When a mode interacts with a thermal reservoir, the evolution of the mode operators  $\hat{a}_k(t)$  and  $\hat{a}_k^\dagger(t)$  also becomes stochastic. As a result, only statistical correlations involving  $\hat{a}_k(t)$  and  $\hat{a}_k^\dagger(t)$  can be predicted for each mode. The correlations obey [20]

$$\begin{aligned}
\frac{d}{dt} \left[ \hat{a}_k^\dagger(t) \hat{a}_k(t+\tau) \right]_R &= -C_k \left[ \hat{a}_k^\dagger(t) \hat{a}_k(t+\tau) \right]_R + C_k \bar{n}(\omega_k) e^{-\frac{1}{2}C_k|\tau|} e^{-i\omega_k\tau} \\
\frac{d}{dt} \left[ \hat{a}_k(t) \hat{a}_k^\dagger(t+\tau) \right]_R &= -C_k \left[ \hat{a}_k(t) \hat{a}_k^\dagger(t+\tau) \right]_R + C_k (\bar{n}(\omega_k) + 1) e^{-\frac{1}{2}C_k|\tau|} e^{i\omega_k\tau}
\end{aligned} \tag{7}$$

where  $[\dots]_R$  denotes the statistical expected value, and  $\bar{n}(\omega_k)$  represents the reservoir energy at frequency  $\omega_k$ . In Eq. (7),  $C_k$  is the mode-reservoir coupling constant, thus  $1/C_k$  represents the cavity damping time. The expected value  $[\hat{a}_k^\dagger(t) \hat{a}_k(t)]_R$  of the photon count decays exponentially with the damping constant  $1/C_k$  toward its steady state value  $\bar{n}(\omega_k)$ , which is usually referred to as the reservoir temperature. Comparing the reservoir characteristic time  $\tau_{\text{reservoir}}$  with the cavity damping time, the mode-reservoir weak coupling condition is  $\tau_{\text{reservoir}} \ll 1/C_k$ . After time  $t \gg 1/C_k$ , the evolution of the correlation, which is described by Eq. (7), reaches steady state, with its behavior described by Eq. (8) below.

$$\begin{aligned}
\left[ \hat{a}_k^\dagger(t) \hat{a}_k(t+\tau) \right]_R &= \bar{n}(\omega_k) e^{-\frac{1}{2}C_k|\tau|} e^{-i\omega_k\tau} \\
\left[ \hat{a}_k(t) \hat{a}_k^\dagger(t+\tau) \right]_R &= (\bar{n}(\omega_k) + 1) e^{-\frac{1}{2}C_k|\tau|} e^{i\omega_k\tau}
\end{aligned} \tag{8}$$

Once mode-reservoir equilibrium has been reached, the correlations on the left hand side of Eq. (8) are fully determined by  $C_k$  and  $\bar{n}(\omega_k)$ .

We next introduce the interaction between the electromagnetic field and a two-level emitter, such as an electron-hole pair in a semiconductor laser. Suppose the emitter is prepared at time  $t = t_0$  in its upper state  $|2\rangle$ . The emitter interacts with the electromagnetic field mode, and the two become quantum mechanically entangled. At some later time  $t > t_0$ , a phase-destroying event occurs, e.g., a collision between two electrons in the conduction band of semiconductors [21]. Such an event either makes the emitter transition to the lower state  $|1\rangle$  while simultaneously adding a photon of frequency  $\omega_{21}$  to the field, or leaves the emitter in the upper state  $|2\rangle$  and the mode with its original photon count. The emitter-mode interaction then begins anew and continues until the next phase-destroying event occurs. When such events are much more frequent than level transitions (transitions between states), the photoemission probability between time  $t_0$  and a later time  $t > t_0$  is small and is given by [22]

$$P_{2 \rightarrow 1}(t) = \frac{1}{\hbar^2} \int_{t_0}^{t_0+t_{\text{coll}}} \int_{t_0}^{t_0+t_{\text{coll}}} \int e^{-i\omega_{21}(t'-t'')} \langle i | (\boldsymbol{\rho}_{12}(\omega_{21}) \cdot \hat{E}_1^*(\mathbf{r}, t')) \cdot (\boldsymbol{\rho}_{12}(\omega_{21}) \cdot \hat{E}_1(\mathbf{r}, t'')) | i \rangle D(\omega_{21}) d\omega_{21} dt' dt'' \quad (9)$$

where  $|i\rangle$  is the initial state of the field, and  $\boldsymbol{\rho}_{12}(\omega_{21})$  is the dipole matrix element.  $\boldsymbol{\rho}_{12}(\omega_{21})$  is a property of the emitter and determines the potential strength of the emitter-mode interaction ([23], §4.3). The actual interaction strength depends on the orientation of the dipole relative to the electric field and is thus governed by the dot product between the two.  $D(\omega_{21})$  is the density of emitter states, which characterizes the inhomogeneity of the system ( $D(\omega_{21}) = \delta(\omega_{21} - \bar{\omega}_{21})$  if all emitters are identical with natural frequency  $\bar{\omega}_{21}$ ). Equation (9) is valid over time intervals short enough such that  $P_{2 \rightarrow 1}(t) \ll 1$ . This condition, known as the emitter-mode weak coupling regime, is met in semiconductors owing to fast phase-destroying intraband collisions, which occur with characteristic frequency  $1/\tau_{\text{coll}} \sim (0.3\text{ps})^{-1}$  at room temperature [6,21]. The photoemission rate is generally much lower, except under very strong applied field and/or very strong spontaneous emission enhancement [4,24]. The opposite limit is the strong-coupling regime, in which neither the emitter nor the field mode experience dephasing events that are more frequent than level transitions; in this situation, Eq. (9) does not apply, and Rabi oscillations result instead [4,25,26]. In this paper, however, we focus on the emitter-mode weak-coupling regime. Equation (9) is therefore employed throughout and evaluated at times  $t = t_0 + \tau_{\text{coll}}$  when, on average, the next phase-destroying collision is expected to occur. To obtain emission probability in free space and in cavities, we evaluate Eq. (9) with the transverse electric field operator of the respective condition.

### 3. Spontaneous emission probability in free space and in cavities

It can be shown from Eq. (9) that photoemission still takes place, with a well-defined probability, even when the mode is in the vacuum state  $|0\rangle$ ; this is referred to as spontaneous emission. We apply Eq. (9) in free space, with all free space modes in the vacuum state and no reservoir present. The field operators in this case have deterministic time dependences described by Eq. (2). By substituting Eqs. (1) and (2) into Eq. (9), we recover the Weisskopf-Wigner probability of spontaneous emission in the limit of a 2-level system when  $D(\omega_{21}) = \delta(\omega - \omega_{21})$  [27],

$$\begin{aligned}
P_{2 \rightarrow 1, |0,0\rangle}^{free} &= \frac{1}{\hbar^2} \int_{t_e}^{t_e+\tau_{coll}} \int_{t_e}^{t_e+\tau_{coll}} \int e^{-i\omega_k(t'-t'')} \langle 0 \dots 0 | \left( \boldsymbol{\rho}_{12}(\omega_{21}) \cdot \sum_{\mathbf{k}, \boldsymbol{\epsilon}} \sqrt{\frac{\hbar \omega_k}{2\epsilon_0 L^3}} \boldsymbol{\epsilon}' \hat{a}_{\mathbf{k}, \boldsymbol{\epsilon}'}(t') e^{i\mathbf{k} \cdot \mathbf{r}_e} \right) \times \\
&\quad \left( \boldsymbol{\rho}_{12}(\omega_{21}) \cdot \sum_{\mathbf{k}', \boldsymbol{\epsilon}'} \sqrt{\frac{\hbar \omega_{k'}}{2\epsilon_0 L^3}} \boldsymbol{\epsilon}'' \hat{a}_{\mathbf{k}', \boldsymbol{\epsilon}'}^\dagger(t'') e^{-i\mathbf{k}' \cdot \mathbf{r}_e} \right) | 0 \dots 0 \rangle D(\omega_{21}) d\omega_{21} dt' dt'' \\
&= \sum_{\mathbf{k}, \boldsymbol{\epsilon}} \frac{\omega_k}{2\hbar \epsilon_0 L^3} \int |\boldsymbol{\rho}_{12}(\omega_{21}) \cdot \boldsymbol{\epsilon}|^2 D(\omega_{21}) R(\omega_k - \omega_{21}, \tau_{coll}) d\omega_{21} \\
&\approx \int \frac{\omega_k^3}{3\pi \hbar \epsilon_0 c^3} \tau_{coll} |\boldsymbol{\rho}_{12}(\omega_{21})|^2 D(\omega_{21}) d\omega_{21}
\end{aligned} \tag{10}$$

In Eq. (10),  $\mathbf{r}_e$  is the location of the emitter, and summation cross-terms cancel owing to  $\langle 0 \dots 0 | \hat{a}_{\mathbf{k}', \boldsymbol{\epsilon}'} \hat{a}_{\mathbf{k}, \boldsymbol{\epsilon}}^\dagger | 0 \dots 0 \rangle = \delta_{\mathbf{k}' \neq \mathbf{k}} \delta_{\boldsymbol{\epsilon}' \neq \boldsymbol{\epsilon}}$ . The

quantity  $R(\omega - \omega_{21}, \tau_{coll}) \equiv \int_{t_0}^{t_0+\tau_{coll}} \int_{t_0}^{t_0+\tau_{coll}} e^{-i(\omega - \omega_{21})(t''-t')} dt' dt'' = \left| \frac{\sin[\frac{1}{2}(\omega - \omega_{21})\tau_{coll}]}{\frac{1}{2}(\omega - \omega_{21})} \right|^2$ , which absorbs

the time exponents inserted from Eq. (2), is the homogeneous broadening function and depends on  $\tau_{coll}$ . Viewed as a function of  $\omega$ ,  $R(\omega - \omega_{21}, \tau_{coll})$  peaks at  $\omega_{21}$ , has a width on the order of  $1/\tau_{coll}$ , and satisfies  $\int R(\omega - \omega_{21}, \tau_{coll}) d\omega = 2\pi \cdot \tau_{coll}$  [16]. The approximation in Eq. (10) consists in replacing the summation over free space modes  $\mathbf{k}$  with appropriate integration and then taking  $\omega_k \approx \omega_{21}$ . Such an approximation is justified because the free space modes form a continuum with an infinitesimal spectral spacing between adjacent modes, and the quantity  $\omega_k^3$  varies little over the width of  $R(\omega - \omega_{21}, \tau_{coll})$ .

A similar procedure can be carried out in an undamped cavity if all cavity modes are initially in vacuum state. Applying Eq. (4) to Eq. (9), summation cross-terms cancel again according to  $\langle 0 \dots 0 | \hat{a}_{\mathbf{k}, \boldsymbol{\epsilon}} \hat{a}_{\mathbf{k}', \boldsymbol{\epsilon}'}^\dagger | 0 \dots 0 \rangle = \delta_{\mathbf{k} \neq \mathbf{k}'}$ , and we obtain

$$P_{2 \rightarrow 1, |0,0\rangle}^{cav} = \sum_k \frac{\omega_k}{\hbar} \int |\boldsymbol{\rho}_{12}(\omega_{21}) \cdot \mathbf{e}_k(\mathbf{r}_e)|^2 D(\omega_{21}) R(\omega_k - \omega_{21}, \tau_{coll}) d\omega_{21} \tag{11}$$

Unlike in free space, the summation over modes  $k$  in Eq. (11) cannot be replaced with integration if the spectral spacing between adjacent modes is non-negligible. This is especially the case in micro- and nano- cavities in which the spacing between adjacent modes may be a significant fraction of the modes' resonance frequencies. The cavity spontaneous emission probability given by Eq. (11) may depend significantly on the number of available modes and their location relative to the density of emitter states  $D(\omega_{21})$ . It also depends on the location and orientation of the emitter relative to the normalized mode field  $\mathbf{e}_k(\mathbf{r})$ . For example, the probability is zero for an emitter located at a field node.

In a damped cavity, the mode interacts with the reservoir. The time dependence of the field operators of a damped cavity is described by the correlation function in Eq. (7). Provided that equilibrium between the mode and the reservoir is reached, we substitute Eq. (8), the steady-state solution of Eq. (7), into Eq. (9) for each cavity mode to obtain,

$$P_{2 \rightarrow 1, \text{equilibrium}}^{cav} = \sum_k \frac{\omega_k}{\hbar} (\bar{n}(\omega_k) + 1) \int |\boldsymbol{\rho}_{12}(\omega_{21}) \cdot \mathbf{e}_k(\mathbf{r}_e)|^2 D(\omega_{21}) \int L_k(\omega - \omega_k) R(\omega - \omega_{21}, \tau_{coll}) d\omega d\omega_{21} \tag{12}$$

where summation cross-terms cancel once again, even though the underlying physics differs from that in Eqs. (10) and (11). In Eq. (12), summation cross-terms cancel because operators of different modes interact independently with the reservoir, and the equilibria are uncorrelated, leading to the evaluation of  $[\hat{a}_{\mathbf{k}'}(t) \hat{a}_{\mathbf{k}}^\dagger(t + \tau)]_R = [\hat{a}_{\mathbf{k}'}(t)]_R [\hat{a}_{\mathbf{k}}^\dagger(t + \tau)]_R = 0$  when

$k' \neq k$ ". Note that we assume the reservoir to be large enough so that the modes do not couple to one another via the reservoir. The Lorentzian  $L_k(\omega-\omega_k)$  in Eq. (12) appears when the damping term in Eq. (8) is expressed as a Fourier transform,

$$e^{-i\omega_k\tau} e^{-\frac{1}{2}C_k|\tau|} = \int e^{-i\omega\tau} L_k(\omega-\omega_k) d\omega, \text{ with}$$

$$L_k(\omega-\omega_k) \equiv \frac{1}{\pi} \frac{\frac{1}{2}C_k}{\left(\frac{1}{2}C_k\right)^2 + (\omega-\omega_k)^2} = \frac{2}{\pi} \cdot \frac{Q}{\omega_k} \frac{\left(\frac{1}{2}\Delta\omega_k\right)^2}{\left(\frac{1}{2}\Delta\omega_k\right)^2 + (\omega-\omega_k)^2}, \text{ where } C_k = \Delta\omega_k \quad (13)$$

and the quality factor is defined as  $Q \equiv \omega_k/\Delta\omega_k$ . The convolution in Eq. (12) determines the emission probability in a cavity for an inhomogeneously broadened ensemble of emitters, when the mode-reservoir equilibrium has been reached. The effect of the reservoir on the emission probability is described by  $L_k(\omega-\omega_k)$ , whose spectral property is described by Eq. (13).

#### 4. Purcell factor in semiconductor lasers

In the remainder of this paper, we apply the results from the non-relativistic QED treatment to a 3-level laser in which emitters are pumped from the ground state  $|1\rangle$  to an excited state  $|3\rangle$  and quickly decay from state  $|3\rangle$  to a lower state  $|2\rangle$ ; the lasing transition is between states  $|2\rangle$  and  $|1\rangle$ . Semiconductor lasers in particular are frequently modeled in this manner, even though their underlying physics differs: state  $|2\rangle$  describes the condition where a conduction band state is occupied and the valence band state of the same crystal momentum is vacant, while state  $|1\rangle$  describes the condition when the conduction band state is vacant and the valence band state is occupied ([28]. §6.3 [29]. §6.2 [30];).

To describe our system, we construct a basic model similar to that in ([20]. §9) and [31]. We suppose each emitter to interact with all modes of the cavity, but ignore direct interaction among emitters. The cavity modes, on their part, undergo damping as a result of loss at the cavity boundaries, and we model the loss as a thermal reservoir.

Loss at the cavity boundary, such as Joule loss in a metallic mirror, or loss of energy through the mirror and its eventual conversion to heat at some remote point in space, generally satisfies the assumptions of a reservoir model: it is weak interaction with a large stochastic system that is disordered and does not retain memory of past interactions. Further, this reservoir is passive, as it does not return energy to the mode. Rather, it drains the mode energy over time, and in steady state  $[\hat{a}_k^\dagger(t)\hat{a}_k(t)]_R = 0$ . Therefore, in Eqs. (8) and (12), we take  $\bar{n}(\omega_k) = 0$ , which is commonly known as the zero temperature condition. The Hamiltonian describing each single emitter in this system can be expressed as

$$\hat{H} = \hat{H}_A + \hat{H}_F + \hat{H}_{AF} + \hat{H}_R + \hat{H}_{FR} \quad (14)$$

where  $\hat{H}_A$ ,  $\hat{H}_F$  and  $\hat{H}_R$  are the emitter, field and reservoir Hamiltonian, respectively.  $\hat{H}_{AF}$  denotes interaction between the emitter and the field modes, while  $\hat{H}_{FR}$  denotes interaction between the field modes and the reservoir.

We note that even if, by assumption, a given emitter does not directly interact with other emitters, the field modes still interact with all emitters present, rather than only with a single emitter. This interaction is not included in the Hamiltonian in Eq. (14), either explicitly or as part of the reservoir. It will be argued in Section 6 that the effect of the emitter population on the field modes cannot justifiably be ignored in semiconductor lasers. However, we adopt the

simplified model as a starting point to illustrate how it leads to the expressions for Purcell factor commonly found in the literature [4,8,11,14,32,33].

In a system where an emitter interacts with the field, and the field interacts with a thermal reservoir, the results summarized in Sections 2 and 3 apply directly. The cavity Purcell factor  $F_{cav}$  is defined as the ratio of spontaneous emission in a cavity to that in free space. In the evaluation of  $F_{cav}$  in the literature, it is common to replace the vacuum free space emission probability presented in Eq. (10) by the emission probability of bulk material of effective index  $n_r$ , with no cavity [4,11]. The spontaneous emission probability in the bulk material,  $P_{2 \rightarrow 1, |0 \dots 0\rangle}^{material}$ , takes the same form as in free space, except that  $\epsilon_{00}$  is replaced by the permittivity of the medium  $\epsilon_r = n_r^2 \epsilon_0$  and that  $c$  is scaled down by the refractive index  $n_r$ . From Eq. (10) we obtain

$$\begin{aligned} P_{2 \rightarrow 1, |0 \dots 0\rangle}^{material} &\approx \int \frac{\omega_{21}^3}{3\pi\hbar\epsilon_r (c/n_r)^3} \tau_{coll} |\boldsymbol{\rho}_{12}(\omega_{21})|^2 D(\omega_{21}) d\omega_{21} \\ &\approx \frac{\bar{\omega}_{21}^3}{3\pi\hbar\epsilon_r (c/n_r)^3} \tau_{coll} |\boldsymbol{\rho}_{12}(\bar{\omega}_{21})|^2 \end{aligned} \quad (15)$$

In the second line of Eq. (15), we evaluate  $\omega_{21}^3$  and  $\boldsymbol{\rho}_{12}(\omega_{21})$  at the center frequency  $\bar{\omega}_{21}$  of the inhomogeneous broadening spectrum  $D(\omega_{21})$  and pull them out of the integration, because these quantities vary relatively little over the homogenous broadening range. Comparing Eqs. (12) and (15), we obtain the Purcell factor  $F_{cav}$

$$\begin{aligned} F_{cav} &\equiv \frac{P_{2 \rightarrow 1, \text{equilibrium}}^{cav}}{P_{2 \rightarrow 1, |0 \dots 0\rangle}^{material}} \\ &= \sum_k \frac{3\pi\epsilon_r (c/n_r)^3}{\tau_{coll}} \frac{\omega_k}{\bar{\omega}_{21}^3} \frac{1}{|\boldsymbol{\rho}_{12}(\bar{\omega}_{21})|^2} \int |\boldsymbol{\rho}_{12}(\omega_{21}) \cdot \mathbf{e}_k(\mathbf{r}_e)|^2 D(\omega_{21}) \int L_k(\omega - \omega_k) R(\omega - \omega_{21}, \tau_{coll}) d\omega d\omega_{21} \quad (16) \\ &\approx \sum_k \frac{3\pi\epsilon_r (c/n_r)^3}{\tau_{coll}} \frac{\omega_k}{\bar{\omega}_{21}^3} \frac{|\boldsymbol{\rho}_{12}(\bar{\omega}_{21}) \cdot \mathbf{e}_k(\mathbf{r}_e)|^2}{|\boldsymbol{\rho}_{12}(\bar{\omega}_{21})|^2} \int D(\omega_{21}) \int L_k(\omega - \omega_k) R(\omega - \omega_{21}, \tau_{coll}) d\omega d\omega_{21} \end{aligned}$$

again evaluating the slowly-varying dipole matrix element  $\boldsymbol{\rho}_{12}(\omega_{21})$  at  $\bar{\omega}_{21}$ . The emission probability in Eq. (12), and hence the Purcell factor in Eq. (16), depends on the location  $\mathbf{r}_e$  of the emitter. More precisely, it depends on the normalized mode field at the location of the emitter  $\mathbf{e}_k(\mathbf{r}_e)$ , as well as on the orientation of the emitter's dipole moment matrix element  $\boldsymbol{\rho}_{12}(\bar{\omega}_{21})$  relative to the field. If the emitters are randomly oriented and uniformly distributed over an active region of volume  $V_a$ , the quantity  $|\boldsymbol{\rho}_{12}(\bar{\omega}_{21}) \cdot \mathbf{e}_k(\mathbf{r}_e)|^2$  is replaced by its average over all locations and orientations.

$$|\boldsymbol{\rho}_{12}(\bar{\omega}_{21}) \cdot \mathbf{e}_k(\mathbf{r}_e)|^2 \rightarrow \frac{1}{3} |\boldsymbol{\rho}_{12}(\bar{\omega}_{21})|^2 \frac{1}{V_a} \int_{V_a} |\mathbf{e}_k(\mathbf{r})|^2 d^3\mathbf{r} \quad (17)$$

where the coefficient 1/3 accounts for the random emitter orientation.

In certain situations, the carrier distribution over  $V_a$  may become non-uniform. For example, in multiple quantum well (MQW) structures, the carrier distributions in the well and barrier regions differ significantly. Even in bulk semiconductors, the recombination of carriers may vary spatially, with the highest rates occurring at field antinodes. This is the case if the recombination at field antinodes is so rapid that diffusion of carriers from other parts of the active volume is not fast enough to avoid depletion. Carrier depletion at field antinodes

and subsequent diffusion from the nodes toward the antinodes leads to the spatial inhomogeneity of the recombination. At room temperature, the diffusion length of carriers in InGaAsP (i.e., average distance traveled before recombination) is on the order of 1-2 $\mu\text{m}$  [34]. The distance between the field node and antinode in visible and near infra-red sub-wavelength semiconductor cavities, on the other hand, is usually less than 0.5 $\mu\text{m}$  [7,8]. Thus, the depletion regions would remain relatively depleted due to the finite diffusion time. Under these circumstances, Eq. (17) should then be replaced by an appropriately weighted average. For the present purpose of illustrating our formulation and avoiding obfuscation of our end goal, we accept the uniform carrier distribution assumption of Eq. (17) and use it in Eq. (16) along with  $e_k(\mathbf{r}_e)$  from Eqs. (5) and (6).

$$\begin{aligned}
F_{cav} &= \sum_k \frac{\pi(c/n_r)^3}{\tau_{coll}} \frac{\omega_k}{\bar{\omega}_{21}^3} \frac{1}{V_a} \left\{ \frac{\varepsilon_r \int_{V_a} |\mathbf{E}_k(\mathbf{r})|^2 d^3\mathbf{r}}{\int \left[ \left( \left. \frac{\partial(\omega' \varepsilon_R(\mathbf{r}, \omega'))}{\partial \omega'} \right|_{\omega'=\omega_k} + \varepsilon_R(\mathbf{r}, \omega_k) \right) \mathbf{E}_k^2(\mathbf{r}) \right] d^3\mathbf{r}} \right\} \times \\
&\int D(\omega_{21}) \int L_k(\omega - \omega_k) R(\omega - \omega_{21}, \tau_{coll}) d\omega d\omega_{21} \quad (18) \\
&= \sum_k \frac{\pi(c/n_r)^3}{\tau_{coll}} \frac{\omega_k}{\bar{\omega}_{21}^3} \frac{1}{V_a} \{ \Gamma_k \} \int D(\omega_{21}) \int L_k(\omega - \omega_k) R(\omega - \omega_{21}, \tau_{coll}) d\omega d\omega_{21} \\
&= \sum_k F_{cav}^{(k)}
\end{aligned}$$

Equation (18) permits several observations. Firstly, the double integral in Eq. (18) is the convolution of inhomogeneous broadening  $D(\omega_{21})$ , cavity Lorentzian  $L_k(\omega - \omega_k)$ , and homogeneous broadening  $R(\omega - \omega_{21}, \tau_{coll})$ . It should be noted that although the homogeneous broadening function  $R(\omega)$  and the inhomogeneous broadening function  $D(\omega)$  appear symmetrically in Eq. (18), they may in principle exhibit different dynamics. In particular, rapid recombination of carriers near the mode frequency  $\omega_k$  may deplete the carrier population at that frequency faster than it is replenished by intraband scattering (this phenomenon is known as “spectral hole burning”). In such cases, it could be meaningful to disaggregate the integral in  $d\omega_{21}$  in Eq. (18) and define separate Purcell factors for carriers at different frequencies  $\omega_{21}$  [35]. More typically, however, especially at room temperatures, the intraband relaxation time  $\tau_{coll} \sim 0.3\text{ps}$  of InGaAsP is much shorter than photoemission time (an assumption already made in Eq. (9)), and the distribution of carriers  $D(\omega_{21})$  is at all times the equilibrium distribution ([23]. Appendix 6). This equilibrium distribution closely resembles the photoluminescence spectrum [36]. In semiconductor lasers utilizing bulk or MQW gain material, it is the broadest of the three convolution factors in Eq. (18) and therefore dominates the convolution. For InGaAsP at room temperature, the full-width-at-half-maximum (FWHM) of  $D(\omega_{21})$  and  $R(\omega - \omega_{21}, \tau_{coll})$  are approximately  $7 \cdot 10^{13}\text{rad/s}$  and  $6.7 \cdot 10^{12}\text{rad/s}$ , respectively.  $D(\omega_{21})$  dominates the convolution in Eq. (18) as long as the cavity Q factor is above 19, which corresponds to a FWHM of  $7 \cdot 10^{13}\text{rad/s}$ . For practical cavities, the Q factor will be significantly larger; thus diminishing the contribution of  $L_k(\omega - \omega_k)$  to the resulting Purcell factor. In fact,  $R(\omega - \omega_{21}, \tau_{coll})$ , alone, dominates  $L_k(\omega - \omega_k)$  if the Q factor is greater than 200 [21,37]. Consequently, in typical III-V semiconductor lasers with MQW or bulk gain material, the cavity Q factor plays a negligible role in determining the spontaneous emission rate and  $F_{cav}$ . Secondly,  $F_{cav}$  may be large in small laser cavities due to its inverse proportionality to the active region volume  $V_a$ . However,  $F_{cav}$  is actually inversely proportional to the effective size of the mode,  $V_a / \Gamma_k$ , where the mode-gain overlap factor  $\Gamma_k$  is defined in Eq. (18) and describes the spatial overlap between the mode and the active

region. Thus if the mode is poorly confined,  $\Gamma_k \ll 1$ ,  $F_{cav}$  will remain small, despite a small active region.

Finally, note that the Purcell factor  $F_{cav}$  is the sum of contributions  $F_{cav}^{(k)}$  from each cavity mode present, as is the emission probability in Eq. (12). However, in the context of nanolasers, greater emission into the mode that would ultimately lase is generally desirable as it helps utilize the carriers more efficiently, whereas emission into other modes is wasteful. From this point of view, therefore, the appropriate figure of merit is not the Purcell factor  $F_{cav}$  but the spontaneous emission factor  $\beta$ ,

$$\beta = \frac{F_{cav}^{(1)}}{\sum_k F_{cav}^{(k)}} \quad (19)$$

where the lasing mode is indicated by the index  $k = 1$ , and the summation is over all modes  $k$ , including cavity modes and modes radiating out of the cavity into free space. The spontaneous emission factor is brought closer to its theoretical limit  $\beta = 1$  when one summation term in Eq. (18) is increased and other terms are suppressed, for example by eliminating unwanted cavity modes [38]. On the other hand, it is worth noting that since the Purcell factor is positively related to the modulation speed of a device,  $F_{cav}$ , rather than  $\beta$  may be the appropriate figure of merit in designing high-speed laser devices [12,13].

## 5. Evaluation of Purcell factor in a sub-wavelength semiconductor laser

In this section, we illustrate the formulation using a semiconductor nanolaser with MQW gain medium, through which we previously demonstrated room temperature laser operation [8]. We use the exact geometry and material parameters of the device as in Fig. 4 of Nezhad et al. [8]. The schematic of the device is depicted in Fig. 1. The key geometrical parameters are the InGaAsP MQW gain core of height  $h_{core} = 480\text{nm}$ , and the major and minor core radii of the slightly elliptical gain (due to fabrication imperfections) are  $r_{major} = 245\text{nm}$  and  $r_{minor} = 210\text{nm}$ , respectively. The  $\text{SiO}_2$  shield layer has thickness  $\Delta \approx 200\text{nm}$ . Assuming the aluminum cladding thickness to be  $70\text{nm}$  (which is twice the skin depth), the height, the major and minor total diameters of this laser are  $1.35\mu\text{m}$ ,  $1.03\mu\text{m}$  and  $0.96\mu\text{m}$  respectively, resulting in a laser cavity that is smaller than its emission wavelength in all three dimensions. The lasing mode of the device, designated  $\text{TE}_{012}$  in [8], is depicted in Fig. 2(a), which is obtained from a COMSOL multiphysics 3D finite element method (FEM) model. The model yields the electric field profile  $\mathbf{E}_{\text{TE}_{012}}(\mathbf{r})$ , mode frequency  $\omega_{\text{TE}_{012}} = 1.330 \cdot 10^{15} \text{rad/s}$  ( $\lambda = 1416\text{nm}$ ), and transparent cavity Q factor  $Q = 479$ , from which the Lorentzian  $L_{\text{TE}_{012}}(\omega - \omega_{\text{TE}_{012}})$  follows via Eq. (13). By transparent, we mean that the permittivity of the gain medium is purely real, and all losses are characterized by the imaginary part of the permittivity of the cavity metal as well as radiation out of the cavity.

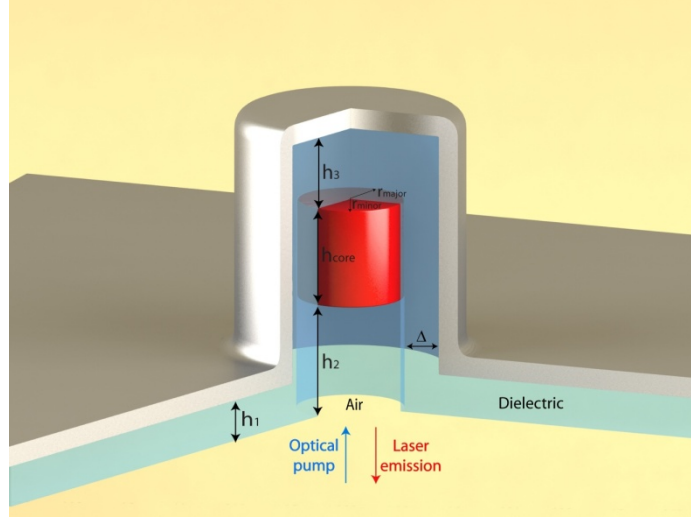


Fig. 1. Schematic of the subwavelength metallo-dielectric laser in Fig. 4 of Nezhad et al. [8]. Key geometrical parameters are  $r_{\text{major}} = 245\text{nm}$ ,  $r_{\text{minor}} = 210\text{nm}$ ,  $\Delta = 200\text{nm}$ ,  $h_1$ ,  $h_2$ ,  $h_3$  and  $h_{\text{core}}$  are 200nm, 550nm, 250nm and 480nm, respectively.

The sinc-like shape of the homogeneous broadening function  $R(\omega - \omega_{21}, \tau_{\text{coll}})$  in Eq. (10) is a consequence of the assumed abrupt dephasing of emitter-field interaction due to an intraband collision at time  $t = t_0 + \tau_{\text{coll}}$ . In reality, the dephasing is not abrupt, and collisions do not happen at precise intervals. Although more accurate lineshape models have been given [21,39,40], it is common to describe homogeneous broadening with a simple Lorentzian, and calibrate the intraband collision time  $\tau_{\text{in}}$  so that  $2/\tau_{\text{in}}$  represents the FWHM of the Lorentzian ([23]. §4.3 [28]. §5.5 [41];). The value of  $\tau_{\text{in}}$  reported in this context is 0.3ps for an InGaAsP MQW at room temperature [6,21]. For our present purposes, the exact shape of homogeneous line broadening is not essential, and we adopt the Lorentzian approximation. The spectra  $L_{\text{TE012}}(\omega)$  normalized to area 1 and  $R(\omega - \omega_{21}, \tau_{\text{coll}})$  normalized to area ( $2\pi\tau_{\text{coll}}$ ) are shown in Fig. 2(b) and Fig. 2(c), respectively.

The origin of inhomogeneous broadening in semiconductors is the quasi-equilibrium Fermi distribution of carriers in the conduction and valence bands, which is maintained through intraband scattering [42]. In bulk material, this distribution can be estimated from the photoluminescence (PL) spectrum. Emission probabilities into the various free space modes  $(\mathbf{k}, \mathbf{\epsilon})$  are given by the summation terms on the second line of Eq. (10): they take the same form as in vacuum modeled classically, except that  $\epsilon_{00}$  is replaced by the permittivity of the medium. The spectrum of this emission is therefore just the convolution  $\int D(\omega_{21})R(\omega - \omega_{21}, \tau_{\text{coll}})d\omega_{21}$ , after neglecting the variation in  $\rho_{12}(\omega_{21})$  over the frequencies involved.  $D(\omega_{21})$  can be recovered from the convolution if  $R(\omega - \omega_{21}, \tau_{\text{coll}})$  is known. For emission into cavity modes, we use the same emitter distribution  $D(\omega_{21})$  as that used for emission into free-space modes. This follows from our assumption that the carrier recombination rate (rate of level transitions) is smaller than the intraband relaxation rate,  $1/\tau_{\text{coll}}$ , which was used to justify the use of Eq. (9). A necessary consequence of this assumption is that spectral hole burning will not occur [6,13]. In the Purcell factor evaluation presented in this section, we use the PL spectrum of the material without the presence of a cavity either measured at low pump powers or as provided by OEpic Semiconductor Inc., who grew the material. The distribution of  $D(\omega_{21})$  is obtained from the PL spectra, which are plotted in Fig. 2(d).

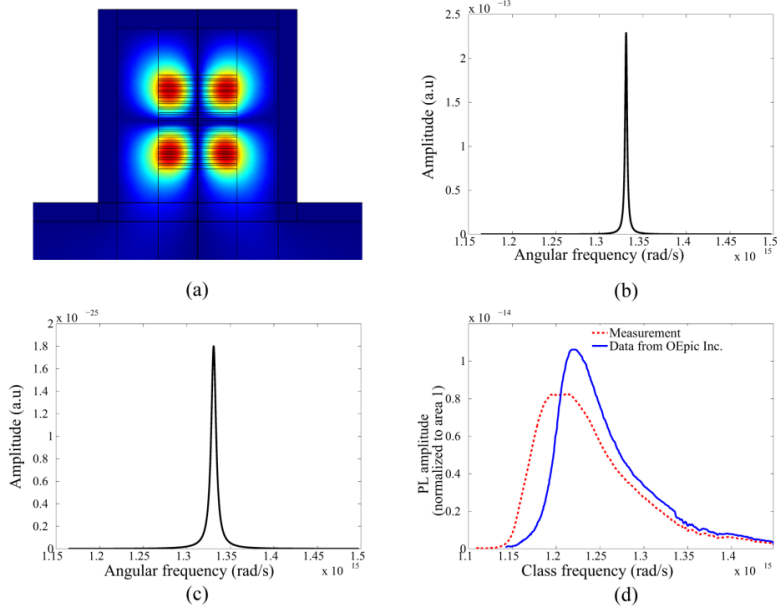


Fig. 2. (a) The lasing mode's electric field profile and the three spectra in the evaluation of the Purcell factor: (b) cavity lineshape, (c) homogeneous broadening lineshape and (d) PL spectra. Dashed red: measured at low pump powers, and solid blue: datasheet provided by OEpic Inc.

Knowledge of the cavity Lorentzian  $L_{\text{TE}012}$ , the homogeneous broadening function  $R(\omega - \omega_{21}, \tau_{\text{coll}})$ , the inhomogeneous distribution  $D(\omega_{21})$  and the field profile  $\mathbf{E}_{\text{TE}012}(\mathbf{r})$  allows us to evaluate the summation term  $F_{\text{cav}}^{(\text{TE}012)}$  in Eq. (18). Table 1 lists the values of  $F_{\text{cav}}^{(\text{TE}012)}$  (sometimes thought of as “single mode Purcell factor”) if material dispersion is neglected, for the following cases: (i) assuming an inhomogeneously broadened gain medium, by evaluating Eq. (18); (ii) ignoring inhomogeneous broadening and assuming instead that all emitters are on exact resonance with the cavity mode, i.e.,  $D(\omega) = \delta(\omega - \omega_{\text{TE}012})$ ; (iii) following the method used in the supplementary material of [8], where both the inhomogeneous and the homogeneous broadening were neglected, i.e.,  $D(\omega) = \delta(\omega - \omega_{\text{TE}012})$  and  $R(\omega - \omega_{21}, \tau_{\text{coll}}) = (2\pi\tau_{\text{coll}})\delta(\omega - \omega_{\text{TE}012})$ . Both homogeneous and inhomogeneous broadenings lower the spontaneous emission rate into mode  $\text{TE}_{012}$ , because, when broadened, not all emitters are on resonance with the  $\text{TE}_{012}$  mode frequency. Further, spontaneous emission from emitters with transition frequencies near the mode resonance in the presence of intraband scattering is less enhanced than that from the same emitters in the absence of intraband scattering. Approximate calculations that do not account for the broadening, such as in [8], may therefore dramatically over-estimate the emission rate and the Purcell factor.

**Table 1. Evaluation of the Purcell factor  $F_{\text{cav}}^{(\text{TE}012)}$  using different methods**

(i) Inhomogeneously and homogeneously broadened	(ii) Homogeneously broadened only	(iii) Unbroadened
0.170 (Measurement)	5.175	8.79
0.215 (OEpic Inc.)		

To compute the spontaneous emission factor  $\beta$  in Eq. (19), it is necessary to evaluate the total spontaneous emission rates in all modes  $k$ , including cavity modes and modes radiating out of the cavity into free space. The Q factors of the radiating modes are low, but their number is large, making a direct summation of terms in Eq. (18) difficult. Alternative

estimation methods exist, based on the formal equivalence between spontaneous emission and the radiation of a classical point dipole [43]. For a cavity such as that of [8], which is not strongly radiating, it may be helpful to obtain the upper bound on  $\beta$  by including in the denominator of Eq. (19) only the cavity modes thought to contribute most to spontaneous emission.

Figure 3 depicts the electric field distribution and  $F_{cav}^{(k)}$  of all the cavity modes with Q factors greater than 20, and whose resonance wavelengths fall within the material PL spectrum of 1300-1670nm. Limiting the summation in the denominator of Eq. (19) to these 5 modes yields the upper bound  $\beta_{max} = 0.359$  using measured PL, and  $\beta_{max} = 0.377$  using PL by OEpic Inc. We note that the geometry of this device is not optimized for maximizing  $\beta$  in the metallo-dielectric cavity design.

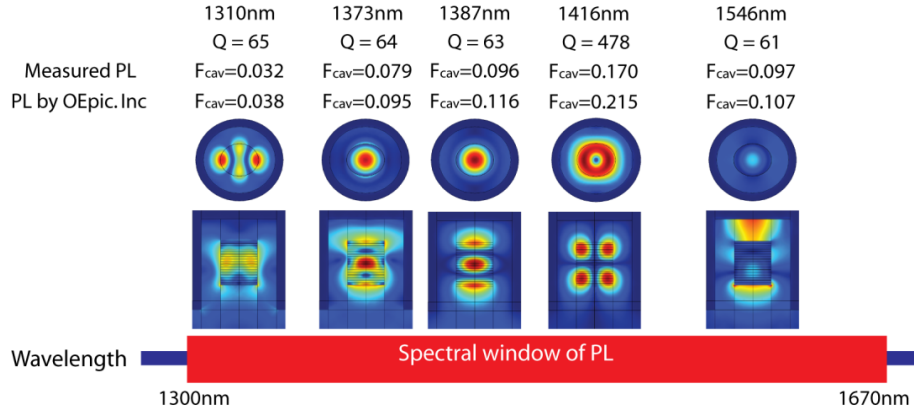


Fig. 3. Simulated mode distribution of all modes that falls within the spectral window of PL and have cavity  $Q>20$ . Also shown are Purcell factors for each mode,  $F_{cav}$ , calculated using two different sources of PL spectra.

## 6. Discussion

In preceding sections, we have summarized the main results of cavity-QED and the quantum theory of damping, and applied these theories to the spontaneous emission in sub-wavelength semiconductor lasers. Consistent application of the theory reveals that some of the intuitions and commonly used formulae originally derived for gas or quantum dot lasers do not carry over to bulk and MQW semiconductor lasers. Two observations are of particular importance.

First, the Purcell factor is often thought to scale as  $Q/(V_a/\Gamma_k)$ , the ratio of cavity Q to the mode volume  $V_a/\Gamma_k$ . In bulk and MQW semiconductors, however, inhomogeneous and homogeneous broadenings typically overwhelm the cavity linewidth, and consequently cavity Q has negligible effect on the spontaneous emission rate. In nanocavities where the cavity modes are sparse and radiation out of the cavity is weak, homogeneous and inhomogeneous broadenings also result in much lower overall spontaneous emission rates than might be the case if all emitters exactly matched the cavity resonance.

Second, in the present model the field-reservoir interaction ( $\hat{H}_{FR}$  in Eq. (14)) includes only losses at the cavity boundary in the form of radiation output and loss through cavity walls. It does not include interaction of the field with the gain material, apart from the single emitter under immediate consideration, which is accounted for in Eq. (14) by the terms  $\hat{H}_A$  and  $\hat{H}_{AF}$ . Consequently, the mode damping constant  $C_k$  in Eq. (8), and the Lorentzian  $L_k(\omega)$  in Eq. (18), describe only cavity wall and radiation loss, and must be computed for a hypothetical structure in which the gain medium (with complex permittivity) is replaced with

a transparent medium (with purely real permittivity). We obtained the Lorentzian in this manner in Section 5, and most authors who report estimates of Purcell factor use the same approach [4,8,11,14,32,33].

Yet even if we accept the assumption, embodied in Eq. (14), that an emitter interacts only with the electromagnetic field modes and does not directly interact with other emitters, these other emitters, just like the cavity boundary, can still modify its emission rate by altering the state of the field modes. The effect of emitters may be less important than that of the cavity boundary in gas lasers and in quantum dot lasers as long as the number of emitters remains small. In bulk and MQW semiconductor lasers, this is not so. Material loss in unpumped InGaAsP at the mode frequency may range from  $3 \cdot 10^3 \text{cm}^{-1}$  to  $10^4 \text{cm}^{-1}$ , depending on the difference between the mode frequency and the material bandgap [44]. If this loss were included, the Q factor of the  $\text{TE}_{012}$  mode in Fig. 2 would drop from the transparent medium value, 479, to as low as 16. The corresponding Lorentzian linewidth would become comparable to the width of the inhomogeneous broadening spectrum  $D(\omega_{21})$ .

While the modification of the modes, and hence of spontaneous emission rates, by the gain medium cannot be ignored, it is also unclear how it can be consistently included in the present model. Unlike the cavity boundary, an unpumped gain medium cannot be treated as a thermal reservoir. Recall that a reservoir must become completely disordered, i.e. a reservoir mode must cycle through all its possible states, over a time  $\tau_{\text{reservoir}}$  that is short relative to the rate of change of the field mode to which it is coupled. For the unpumped gain medium, the dephasing time scale  $\tau_{\text{reservoir}}$  would be on the order of  $\tau_{\text{coll}} \sim 0.3 \text{ps}$ . Yet the damping it inflicts on the mode is so severe that the mode decays in as little as  $0.012 \text{ps}$  (based on  $Q = 16$  and  $\omega = 1.330 \cdot 10^{15} \text{rad/s}$ ). Under such strong damping, even the treatment of the cavity boundary as a thermal reservoir becomes questionable, although the electron collision time in metals is on the order of  $0.01 \text{ps}$  [45,46].

It is also worth noting that once pumping is introduced, the (classically defined) Q factor of the mode rises and reaches a theoretical value of infinity at the lasing threshold. It seems likely that, in the quantum mechanical treatment, the manner in which the gain medium modifies the mode and, through the mode, modifies the emission rates, would also change as pumping is added. In this situation, however, the gain medium conforms even less to the thermal reservoir model, for it is no longer at equilibrium with the mode, and so Eq. (8) cannot be used. Furthermore, as pumping is increased and the field builds up in the cavity, the transition rate grows and may eventually exceed the collision rate, violating the emitter-mode weak coupling condition,  $P_{2 \rightarrow 1}(t) \ll 1$ . Under this circumstance, Eq. (9) can no longer be used. Intuitively, one may expect the gain material to partly compensate the dissipation at the cavity boundary, while at the same time contribute randomness to the mode state through spontaneous emission. Formal quantum mechanical treatment of the Purcell effect in semiconductor lasers, incorporating the effect of the gain medium, is the subject of future research.

## Acknowledgments

The authors would like to thank Dr. Aleksandar Simic for helpful discussions. This work was supported by the Defense Advanced Research Projects Agency (DARPA), the National Science Foundation (NSF), NSF through Center for Integrated Access Networks (CIAN) NSF ERC under grant #EEC-0812072, the Cymer Corporation, and the U.S. Army Research Office. This work was also partly supported by the Brazilian financial agencies: FAPESP, CNPQ, CAPES and done within the National Institute for Science and Technology (FOTONICOM) and the Center for Optics and Photonics (CePOF).